Optics and Lasers in Engineering 107 (2018) 231–240

Contents lists available at ScienceDirect

Optics and Lasers in Engineering

journal homepage: www.elsevier.com/locate/optlaseng

Mode matching of Continuous Scanning Laser Doppler Vibration data in the frequency domain

P. Chiariotti[a,*], M. Martarelli[b], P. Castellini[a]

[a] Università Politecnica delle Marche Politecnica delle Marche, Via Brecce Bianche, Ancona 60131, Italy
[b] Università degli Studi e-Campus, Via Isimbardi, Novedrate (CO), Italy

ARTICLE INFO

Keywords:
Laser Doppler Vibrometry
Continuous Scanning Laser Doppler Vibrometry
Pattern matching
Dynamic testing
Mechanical measurements

ABSTRACT

Applications as structural diagnostics, condition monitoring and fatigue testing are requiring the development of vibration tests characterized by reduced testing time, fine spatial resolution and high Signal to Noise Ratio (SNR). In this context, Continuous Scanning Laser Doppler Vibrometry (CSLDV) can have a great impact as a substitute of classic Discrete Scanning Laser Doppler Vibrometry (SLDV). In fact, CSLDV makes it possible to measure the target structural vibration much faster and with finer spatial resolution than SLDV, as well keeping an acceptable level of SNR. CSLDV joins together the spatial and time information, because the vibration datum obtained from the laser, which continuously scans (over time and space) the structure under test, is modulated by the Operational Deflection Shape (ODS) excited during the experiment. This results in a spectrum characterized by sideband patterns uniquely associated to the ODS excited. However, the current drawback in fully exploiting CSLDV in everyday testing is related to the necessity of being managed by an expert operator who knows how to extract meaningful information from data measured. This paper proposes a procedure which aims to automatize the information extraction process from CSLDV signals, in order to ease the utilization of CSLDV in vibration laboratories. The idea starts from a simple observation: if the mode shapes of the structure under test are known a priori, e.g. from a numerical model, an analytical formulation or previous measurements, as is the case for fatigue tests, it is possible to settle a procedure that searches for similarities between those known mode shapes (the candidate mode shapes) and ODSs that actually modulate the signal measured. This procedure can therefore be considered a pattern matching technique that is able to identify the resonance frequency related to each ODS and the mode shapes that better match with the ODSs excited. A detailed description of the algorithm is given in this paper. Moreover, the procedure is analyzed in order to discuss its sensitivity to noise, overlapping of resonance frequencies (close modes situation) and ODS complexity. The application of the approach to experimental data is also discussed.

1. Introduction

Speeding up the testing time and keeping a fine spatial resolution are becoming key requirements in vibration-based tests for applications like structural diagnostics, condition monitoring and fatigue testing. Moreover, very often, in these applications, the processing method relies on the comparison between an a-priori status of the target structure (e.g. the undamaged status) and the current one, so to associate any deviation to a structural modification (e.g. thus indicating the presence of a damage). Discrete Scanning Laser Doppler Vibrometry (SLDV) has been used a lot for this purpose during the last ten years, since it gives the possibility to analyze a structure contact-less, with a very fine spatial resolution and keeping a high Signal to Noise Ratio (SNR). In Discrete SLDV the laser spot is steered on a point of the target surface by exploiting automated mirrors; the measurement is performed on that point and then the laser is moved to another point. This process repeats until a scan over the target area is completed. Testing time is therefore related to the spatial resolution (spatial distance between two consecutive points) with respect to the area to be scanned. This is the main drawback of the approach. Indeed, if an extremely fine spatial resolution is sought, testing time can increase exponentially, and the structure itself can modify its behavior during the test duration.

The Continuous Scanning Laser Doppler Vibrometry (CSLDV) method entered in the vibration testing measurement community as an alternative to conventional Discrete Scanning Laser Doppler Vibrometry (SLDV). Its main appeal is related to the reduced testing time, since the laser spot is continuously moved over the target surface while acquiring vibration data. This makes it possible to collect time and spatial data simultaneously, utilizing a spatial resolution that depends on the sampling frequency adopted during the measurement. Original efforts in

* Corresponding author.
E-mail address: p.chiariotti@univpm.it (P. Chiariotti).

https://doi.org/10.1016/j.optlaseng.2018.03.034
Received 8 August 2017; Received in revised form 18 February 2018; Accepted 27 March 2018
Available online 7 April 2018

CSLDV relate to experiments by Sriram et al. [1] in extracting Frequency Response Functions using broadband excitation and synchronous sampling at the laser scan speed. However, the major contributions to the development of this measurement technique are due to Stanbridge et al. [2,3], who proposed to extract mode shapes exploiting the amplitude modulation effect induced by the ODS of the structure on the time vibration signal collected when the laser scans continuously (at scan rates independent to the sampling frequency) the target surface. Initially, this method was proposed for near-resonance excitation conditions, e.g. step sine testing, with the drawback of being quite time demanding. Over the years several researchers have kept working on CSLDV for extracting ODS, highlighting its good performances even in case of broadband excitation, e.g. impact testing [4], broadband [5] and operational excitation [6,7]. Different approaches have been developed, as the lifting approach proposed by Allen [8–10], which exploits high scanning rates to rearrange data collected at each point along the scan path as they were measured in Discrete Scanning mode. Alternative use of CSLDV can be cited for vibro-acoustic applications [11], damage detection [12], moving targets [13] and biomedical applications [14]. A multi-beam CSLDV approach was also proposed by Aranchuk et al. [15] for land-mine detection.

The key feature of a CSLDV measurement is that the time history acquired appears as an amplitude modulated signal, whose modulation is due to the Operational Deflection Shapes excited. As suggested by Ewins et al., an ODS can be modeled by a polynomial, whose coefficients are directly related to the sidebands that characterize the vibration spectrum of the CSLDV signal. The sidebands around the resonance frequency of a specific ODS are spaced by the laser beam scanning frequency, while the number of sidebands are directly related to the ODS spatial complexity. Conventionally, the recognition of resonance frequencies and the recovery of ODSs in the processing of CSLDV data are performed starting from the observation of the CSLDV output spectrum. This process has obviously to be performed by an expert experimenter used to treat with CSLDV data. Some years ago Chiariotti et al. [16] presented a new philosophy for CSLDV data processing that reverses this approach. Indeed, their *mode-matching processing* starts form this observation: if a specific ODS produces a unique sideband pattern, then the identification of that pattern within the CSLDV spectrum, in a pattern matching-like approach, proves that the same ODS was excited during the test. It is then possible to create a set of sideband patterns starting from a set of ODSs (e.g. obtained theoretically, numerically, experimentally, etc.) and look for those patterns within the CSLDV spectrum. Those patterns that are recovered in the spectrum correspond to the candidate shapes that better match with the ODSs that effectively modulate the CSLDV signal. The procedure, therefore, does not extract neither ODSs nor mode shapes, but indicates which ODSs, among those excited, best resemble those constituting the set of candidate shapes. In this sense, it is not inappropriate to state that the candidate shapes can be both mode shapes (e.g. obtained analytically or numerically) and ODSs (e.g. obtained experimentally from previous measurements, as it can happen in fatigue testing).

The implication of this approach on applications such as condition monitoring/diagnostics, fatigue testing, etc. is straightforward. Indeed, if a structure undergoes to structural modification because of the presence of a damage/defect, the approach can be exploited to check whether the sideband patterns of the undamaged target are still present in the CSLDV vibration spectrum. Any fail in identifying the patterns associated to the undamaged structure might suggest a structural modification. The advantage with respect to a classic Discrete SLDV approach, where modal variations are looked for, is in the possibility to carry on the test in a much shorter time improving the spatial resolution, as well keeping an acceptable level of SNR. The spatial resolution aspect is particularly important, since a finer spatial resolution increases the probability to get vibration data over the damaged area.

The paper is organized as follows: Section 2 describes the proposed method. Section 3 aims to discuss the sensitivity of the approach to the three phenomena that mainly interfere with a correct identification of the patterns, i.e. Signal to Noise Ratio (SNR), sideband spectra overlapping and ODS complexity. Section 4 describes the results obtained when utilizing the approach on real test cases, while Section 5 draws the main conclusions of the work.

2. Mode matching procedure in frequency domain

The aim of the method proposed in this paper is to exploit an a-priori knowledge of mode shapes or ODSs, which can be known from any other approach such as numerical, analytical models, previous experimental testing, etc., to create a set of virtual sideband patterns to be looked for in the CSLDV spectrum. Those virtual patterns that best match with those effectively present in the CSLDV spectrum make the labeling of modes and ODSs possible. In practice, this technique emulates and reverses what an expert experimenter usually does when analyzing CSLDV data. Indeed, the experimenter looks for a sideband pattern in the CSLDV spectrum and recovers the ODS from this pattern. The proposed approach starts with the creation of a database in which each mode shape/ODS is identified as a sideband pattern. Once this data base is created, a pattern matching procedure in the CSLDV spectrum is started. In such a way, the pattern that best matches within the CSLDV spectrum indicates that an ODS, similar to the corresponding mode shape/ODS that produced that pattern, was excited during the test. The output of the procedure consists of:

- the resonance frequencies corresponding to the central frequencies of the sideband pattern better matching with the candidate ones,
- a set of mode shapes that best matches with the ODSs that effectively modulate the CSLDV signal measured.

A clarification is needed. This mode matching procedure makes it possible to identify the candidate shapes that better match with those ODSs that effectively modulate the CSLDV signal. This procedure does not extract neither ODSs nor mode shapes, it identifies and labels which ODSs, among those excited, best resemble those constituting the initial data base. In this sense, it is not inappropriate to state that the shapes populating the initial database can be both mode shapes (e.g. obtained analytically or numerically) and ODSs (e.g. experimentally obtained).

A detailed description of the mode matching procedure is reported hereafter.

2.1. Step1: CSLDV data collection

The first step of the approach consists in collecting vibration data utilizing CSLDV. The laser spot is moved continuously along the whole length of the target (any kind of scan path can be exploited) and the vibration velocity of the target is measured. As a result of this continuous movement of the laser spot, the vibration time history ($v_z(t)$) is amplitude modulated by the ODSs excited.

2.2. Step 2: creation of shapes database

A database containing mode shapes/ODSs is created. These shapes can be calculated analytically or via numerical models (e.g. FE models), can be the result of a model updating procedure, or can be arbitrarily picked from previous experiments on the same structure (e.g. as it can happen in fatigue testing or in structural diagnostics). Just to make an example, if we are experimentally dealing with a clamped-free beam, the mode shapes filling the shapes database can be defined analytically using the formulation proposed in [19]:

$$X_i = \left[cosh\left(\lambda_i \frac{x}{L}\right) - cos\left(\lambda_i \frac{x}{L}\right)\right] - \sigma_i\left[sinh\left(\lambda_i \frac{x}{L}\right) - sin\left(\lambda_i \frac{x}{L}\right)\right] \quad (1)$$

where x is the coordinate position along the beam length L, while λ_i and σ_i are the non-dimensional frequency amplitude parameters. Moreover, since the actual constraint of a structure can be partially known or even unknown, it is plausible to insert, in the shapes database, modes that are obtained with different types of constraints (e.g. pinned-free, etc.).

2.3. Step 3: sideband spectrum kernel synthesis

The basic assumption of the procedure is that each candidate shape can be fitted, in general sense, by a two-dimensional polynomial series of degree p, q and coefficients $V_{R_{n,m}}$, $V_{I_{n,m}}$:

$$V_R(x,y) = \sum_{n,m=0}^{p,q} V_{R_{n,m}} x^n y^m; V_I(x,y) = \sum_{n,m=0}^{p,q} V_{I_{n,m}} x^n y^m. \quad (2)$$

The vibration velocity, translated to a two-dimensional structure, results in

$$\hat{v}_z(x,y;t) = V_R(x,y)\cos(\omega t) + V_I(x,y)\sin(\omega t) \quad (3)$$

where ω represents the frequency. This polynomial modulates the amplitude of the time history obtained from a CSLDV measurement, as reported in Eq. (4), where Ω_x and Ω_y represent the scan frequencies in x and y directions.

$$\begin{aligned}\hat{v}_z(t) = &\sum_{n,m=0}^{p,q} V_{R_{n,m}} \cos^n(\Omega_x t)\cos^m(\Omega_y t)\cos(\omega t) \\ &+ V_{I_{n,m}} \cos^n(\Omega_x t)\cos^m(\Omega_y t)\sin(\omega t)\end{aligned} \quad (4)$$

This expression can be related to the sidebands of the CSLDV spectrum by the following formulation:

$$\hat{v}_z(t) = \sum_{n,m=0}^{p,q} A_{R_{n,m}} \cos\left[(\omega \pm n\Omega_x \pm m\Omega_y)t\right] + A_{I_{n,m}} \sin\left[(\omega \pm n\Omega_x \pm m\Omega_y)t\right]. \quad (5)$$

The real and imaginary coefficients (A_R and A_I) of the sidebands characterizing the spectrum of this vibration signal are related to the polynomial coefficients V_R, V_I by means of the Chebyshev matrix $[T]^{-1}$, [2], in accordance to:

$$\{A_R\} = [T]^{-1}\{V_R\}[T], \{A_I\} = [T]^{-1}\{V_I\}[T]. \quad (6)$$

The pattern of these sidebands (the *kernel*) uniquely identifies a shape, and therefore it can be exploited as the template for a pattern matching procedure (see Section 2.4) that aims to identify the presence of that shape in the spectrum of the CSLDV vibration signal. Each kernel is reconstructed from the sideband amplitude coefficients, obtained from A_R and A_I, according to:

$$A = \sqrt{(A_R{}^2 + A_I{}^2)}. \quad (7)$$

Even though the shapes in the database can be amplitude normalized when they are obtained, for instance, from analytical equations as Eq. (1), the corresponding sideband spectrum is not. This happens because the energy of the mode shape is spread over several sidebands, see Fig. 1. It is thus clear that, increasing the spatial complexity of the shape, which means considering mode shapes of higher spatial order, the number of sidebands increases and the amplitude of the kernel decreases accordingly.

2.4. Step 4: sideband spectra matching

Each kernel associated to a shape in the database is then compared with the CSLDV amplitude spectrum in a pattern matching-like procedure. The matching rule is based on the minimization of the Euclidean distance d_i between a template (each kernel) and the CSLDV amplitude spectrum. The method is based on the sliding window approach, that is a typical brute force method in Time-series Subsequence Matching [17,18].

$$d_i = \left\| \frac{K}{max(K)} - \frac{W_i}{max(W_i)} \right\| \quad (8)$$

where

K	is the kernel associated to a particular shape of the database
$W_i = S(i : \frac{\Omega_s}{d_f} : i+N)$	is the sliding window of the CSLDV signal amplitude spectrum S
$\|\|.\|\|$	represents the L_2 Euclidean distance
N	is the number of spectral lines of the kernel K
M	is the number of spectral lines of the signal amplitude spectrum S
$i = 1 : M$	represents the position (frequency) of the sliding window
$max(K)$	is the maximum value in the kernel K
$max(W_i)$	is the maximum of the amplitude spectrum S within the i^{th} window of length N
Ω_s	represents the scan frequency/frequencies (in case of 2D scanning) adopted in the CSLDV measurement
d_f	is the frequency resolution adopted in the CSLDV measurement

The sliding window W_i is extracted from the whole spectrum and compared with the template (kernel). The distance metric (Euclidean) is stored and the sliding window is shifted ahead by one spectral line. Only the amplitude values at the discrete spectral lines that are multiples of Ω_s are considered in the sliding window when calculating the distance to the kernel. Indeed, these are the only significant lines that contain the information related to the ODSs. Moreover, this approach both improves the computational effort and makes the procedure less sensitive to noise, as it will be further explained in Section 3.1.

There might also be cases in which the scan frequency is high and the first natural frequency is low. When this happens, negative sidebands fold back to the positive axis. Typically, to avoid this issue, it is good practice to set the scan frequency to be lower than 1/5 of the first natural frequency of the structure under test. However, the algorithm takes this issue into account by modifying the sideband pattern so that the negative sidebands fold back in the positive axis.

Once the all amplitude spectrum is scanned, the sliding window showing the minimum distance for a certain kernel is identified and the central frequency of that window extracted accordingly. The procedure is repeated for the whole shapes filling the database. The labeling, i.e. the identification of significant ODSs in the CSLDV spectrum and the consequent association to a specific shape in the database, is performed on the basis of the values of Eq. (8). The lower the Euclidean Distance, the higher probability the selected shape has to represent an ODS excited on the target structure.

3. Sensitivity analysis

The algorithm has been tested on simulated data in order to understand its sensitivity to three factors:

- Signal to Noise Ratio (SNR); in CSLDV measurements noise has a double nature, random and periodic. The latter, which produces unwanted frequency components at the laser beam scan frequency/frequencies and its/their harmonics, is mainly due to speckle noise;
- sideband spectra overlapping: this is a situation that can happen when uncoupled-close mode shapes are excited;
- ODS complexity, e.g. when the ODS modulating the LDV signal is a combination of two or more mode shapes: this can happen in complex structures with coupled-close mode shapes.

The vibration signal virtually measured by CSLDV on a clamped-free cantilever beam was modeled. The synthesized signal was obtained simulating a sampling frequency of 10 kSamples/s for a total observation period of 10 s. A scanning frequency of 1 Hz was adopted, while the scan path was chosen as a sinusoidal line path centered at the center of the beam length (L=2 arbitrary units -a.u.) in the vertical direction (direction addressing the constraint-to-free tip direction). A different number of mode shapes, all calculated according to Eq. (1), were involved in the synthesis process. This choice was related to the phenomenon to be investigated, as it will be explained in the following. The first resonance frequency, i.e. the one characterizing the first bending mode,

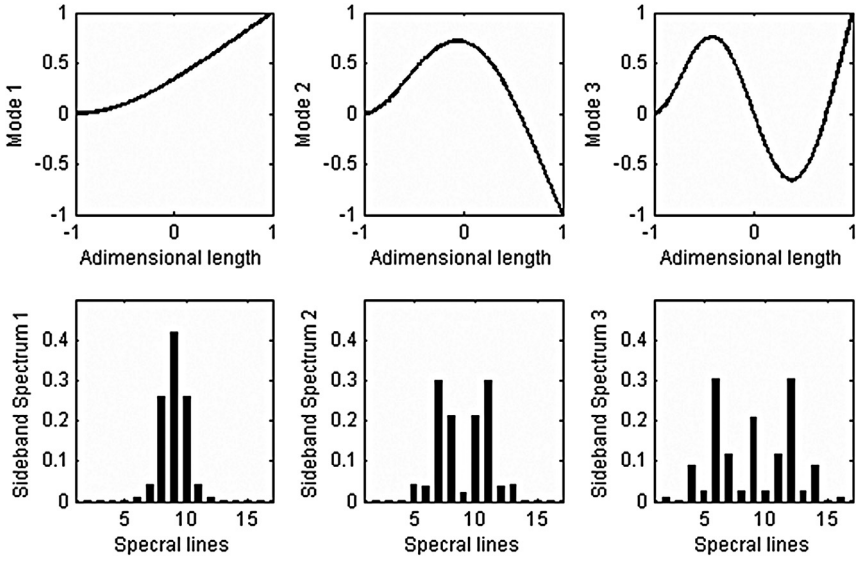

Fig. 1. Sidebands spectra associated to mode shapes for a clamped-free beam.

was chosen to take place at 40.2 Hz, while the frequencies associated to the following modes were chosen according to the mode shapes progression described in [19]. A damping ratio of 0.1 was also adopted for each mode. These choices have no influence on the generalization of the whole approach.

3.1. Mode extraction vs noise

A real signal is always affected by noise. This is particularly true in LDV testing, where the experimenter has to deal also with speckle noise. In fact, when laser light, which has a coherent nature, impinges on an optically rough surface, the grains constituting this surface dephase the light returning to the detector, causing constructive and destructive interference that result in bright and dark regions over the detector area. This pattern, known as speckle-pattern, evolves during the relative motion between the laser spot and the surface, thus giving rise to pseudo-vibrations that are difficult to distinguish from the true vibration. This phenomenon gets worse when the laser spot continuously moves over the target surface as it happens during a CSLDV measurement. In fact, the speckle pattern evolves in tuning with the relative movement between the target and the laser spot, and a series of different bright speckles move in front of the detector area, thus producing a pseudo-random change in the speckle phase distribution. If the laser beam moves along a straight line reproducing a perfect sinusoidal pattern, the speckle grains will pass across the detector active area with the same frequency as the scanning beam, thus introducing frequency components at the scan frequency and its harmonics [20]. The overall SNR therefore decreases because the increase in the total Harmonic Distortion (THD) at the scan frequency. Speckle noise has also a random component, which might be due, for instance, to small deviations with respect to a scan path perfectly repeating itself. This component resulted to be less important than the periodic one, as demonstrated by Sracic et al. in [21]. Apart from speckle noise, noise linked to the whole measurement chain, which is expected to be random in nature, might be present in the signal.

A dedicated analysis was performed to test the sensitivity of the full approach to these two types of noise (periodic speckle noise and random noise). Only the first bending mode of the cantilever beam was involved in building the synthesized signal previously described. Periodic noise at the laser beam scan frequency and its harmonics was added to the noise-free CSLDV signal. The SNR level was made to vary from -20 dB up to 20 dB with 1 dB step. The amplitude of the periodic noise was varied randomly under the constraint of keeping the SNR at the desired level. In order to provide statistical meaning to the data generated, 128 trials were performed for each SNR value. For each case, the Euclidean distance between the kernel and the signal was calculated. The average distance and its standard deviation bounds are plotted in Fig. 2 (a), showing that the mode shape is recognized when the distance goes towards zero, right part of the plot. In that case the standard deviation decreases to zero as well. The limit after which the mode shape is not recognized any more is given by the vertical black line, that is at about 0 dB. The vertical gray lines represent the standard deviation bounds with respect to the recognizability limit. Below that limit the mode shape is not identified and the Euclidean distance remain constant at a value far from zero.

The same approach was used for testing the algorithm sensitivity to random noise, see Fig. 2(b). In this case the SNR limit is lower, e.g. about −17 dB, although the lower standard deviation bound of the recognizability limit is close to −20 dB. Another interesting point can be extracted form this analysis. It seems plausible to consider 0.85 as a reasonable threshold of the Euclidean distance for a correct identification of the shape. This threshold is the one which will be effectively utilized in the next sections to confirm that a certain shape is correctly identified in the CSLDV signal. Globally, it can be stated that, as it was expected, the algorithm is more sensitive to periodic noise than to random noise, because periodic noise generates frequency components at the laser beam scan frequency and its harmonics that can modify the sideband pattern within the signal when the ODS central frequency is an integer multiple of the scan frequency. This is the worst case scenario of a measurement performed by CSLDV and that is why this situation was considered in the simulation. In case where the central frequency is not an integer multiple of the scan frequency, the algorithm is completely unaffected by periodic noise, since the sideband pattern remains unaltered.

3.2. Mode extraction vs sideband patterns distance

In order to test the sensitivity to uncoupled-close mode shapes, and thus both to close resonance frequencies and overlapping sidebands, the virtual CSLDV signal reproducing the vibration of the clamped-free cantilever beam described in Section 3 was created in order to involve only the first two vibration mode shapes. However, while the resonance frequency of the first mode was kept fixed at 40 Hz, the resonance frequency of the second mode shape was varied each time, with a step

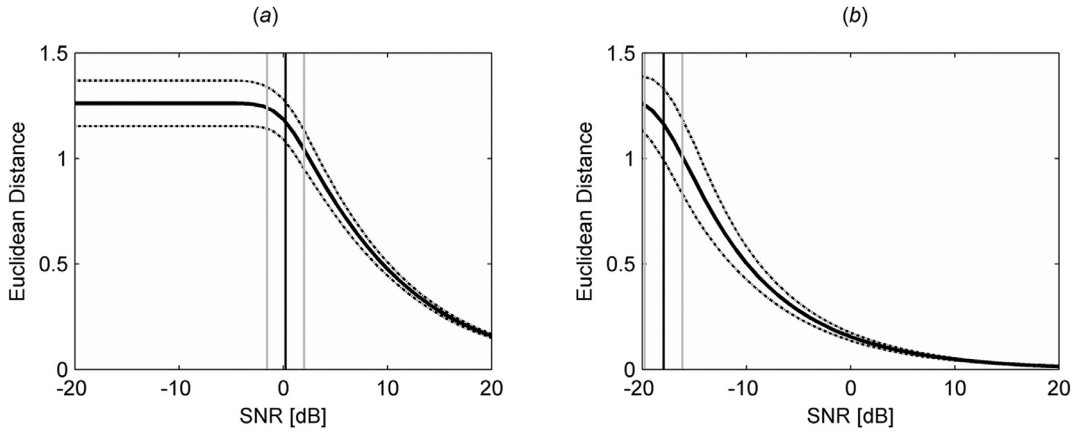

Fig. 2. Sensitivity of the approach to SNR: Euclidean distance $_{vs}$ SNR for periodic noise (a) and random noise (b).

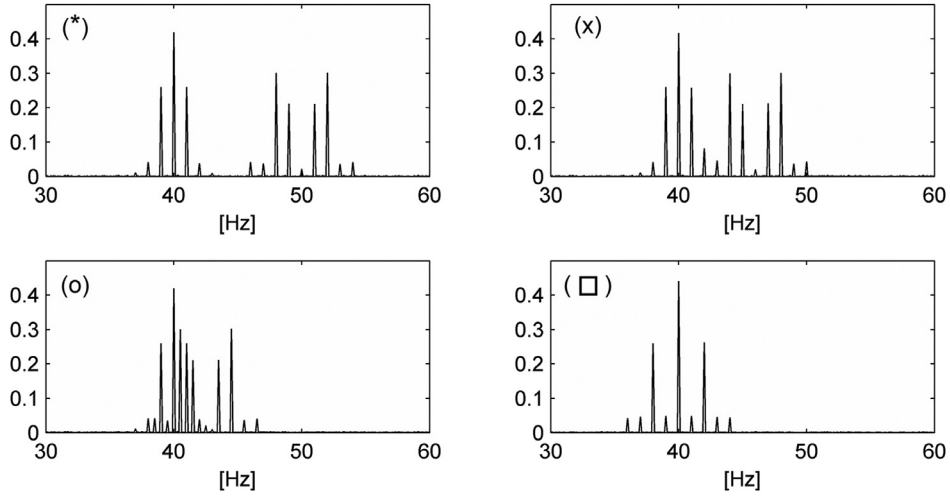

Fig. 3. Sensitivity of the approach to sideband patterns distance: Synthesized sideband spectra at different central frequency difference between the two mode shapes.

equal to the frequency resolution used for synthesizing the signal, in order to get it closer to the resonance frequency of the first mode shape. This action made the sideband patterns that characterize the two mode shapes to pass through different conditions, from well separation (difference between central frequencies of around 40 Hz) to closeness, up to overlapping (this latter with different ranges of severity).

As long as the central frequency of the two sideband patterns are sufficiently far apart, e.g. up to a frequency difference of 10 Hz, the resonance frequency for both mode shape I and mode shape II are correctly identified. When the central frequency difference is 10 Hz (*) the first sideband of the sideband spectra coincides, see top left plot of Fig. 3. In that case the central frequency identified for mode shape II is wrong (with an error of 100 Hz) because its sideband spectrum contains high order sidebands which give an important contribution to the mode shape reconstruction. The central frequency of mode shape I, instead, is correctly recognized (i.e. error of 0 Hz) because the significant sidebands are limited to lower order. When the difference between the two central frequencies decreases, the error in identifying the resonance frequency of both the mode shapes increases, up to 80 Hz for mode I and 200 Hz for mode II. This happens because the sideband spectra are completely overlapping, see top right plot of Fig. 3 where the central frequency difference is 6 Hz (x). However it can be noticed, from the characteristic shape of the error plot, that when the sideband pattern of mode I and the sideband pattern of mode II do not coincide (between the peaks) the resonance frequencies of both modes are correctly estimated (i.e. error of 0 Hz), see bottom left plot of Fig. 3 where the central frequency difference is 2.6 Hz (○).

When the two mode shapes central frequency difference goes below the frequency resolution of the experiment, namely 0 Hz (□) a limiting case is reached. The sideband pattern results in a combination of the two sideband patterns, as can be seen on the bottom right plot of Fig. 3, and therefore to a mode shape that is neither mode I nor mode II. However the algorithm attributes that sideband pattern to the mode shape having the most similar sideband pattern, i.e. mode I in this case.

Fig. 4 summarizes the trend of the error in the identification of the correct resonance frequency of each mode shape, e.g. the difference between the resonance frequency assigned to each mode shape and the central frequency attributed by the algorithm to that mode shape, in relation to the difference Δf_c between the two central frequencies of the two mode shapes used to synthesize the signal. The top plot shows the trend for mode shape I and the bottom plot the trend for mode shape II.

3.3. Mode extraction vs ODS complexity

Very often the ODS modulating the CSLDV signal can be a combination of several modes, as it can happen for complex structures with close-coupled modes. A virtual CSLDV signal was thus synthesized considering, as modulating ODS, a mode shape that is progressively morphing into another one. Considering the first two mode shapes of the cantilever beam, mode I and mode II, shown in bottom left and right plot of Fig. 5, the signal has been synthesized starting with the single contri-

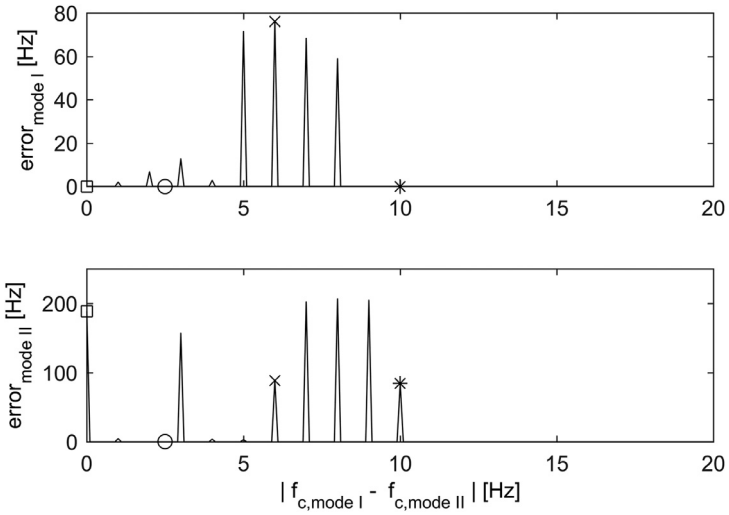

Fig. 4. Sensitivity of the approach to sideband patterns distance: Resonance frequency error $_{vs}$ central frequency difference between the two mode shapes for mode shape I (top plot) and mode shape II (bottom plot).

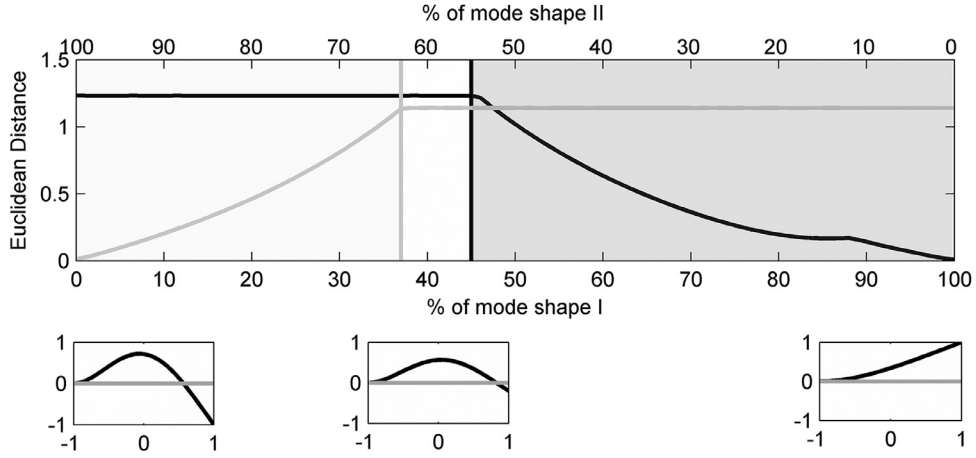

Fig. 5. Sensitivity of the approach to ODS complexity: Euclidean distance $_{vs}$ mode shape complexity.

bution of mode I and progressively adding the contribution of mode II while decreasing the contribution of mode I, according to the following equation:

$$ODS = w * mode_I + (1 - w) * mode_{II} \quad (9)$$

were w is a weighting factor ranging from 0 to 1. The complex ODS where the two mode shapes coalesce (for a given combination of mode I and mode II) is shown in the bottom central plot of Fig. 5. It should be noted that the value of the resonance frequency has little/no importance in this test, since the aim is to verify the response of the approach to spatial degradation of mode shapes.

The algorithm recognizes mode I (dark gray area) as long as the ODS is a combination of 45% of mode I (black line) and 55% of mode II. Mode II is recognized as long as the ODS is a combination of 63% of mode II and 37% of mode I. In the region between 37% and 45% of mode I (i.e. the complement for mode II) neither mode I nor mode II are recognized, i.e. the Euclidean distance is higher than 1 for both the modes.

4. Application to experimental data

4.1. Mutli-sine excitation test

In order to demonstrate the capabilities of the proposed technique, an experimental test has been performed on an aluminum clamped-free cantilever beam (height=0.3 m; width=0.03 m; depth=0.004 m).

Table 1
Resonance Frequencies of the tested clamped-free cantilever beam: Multi-sine excitation.

Mode shape	Resonance Frequency [Hz]
I	40.6
II	243.3
III	665.5
IV	1293.5

The beam was excited to vibrate to bending modes by an electrodynamic shaker connected to the beam close to the clamping constraint (Fig. 6). The laser was placed (z_0) 2 m apart from the beam. This relative target-to-laser distance aimed to keep the initial speckle noise sufficiently low. This aspect was well demonstrated by Sracic and Allen [21], who showed that increasing the target-to-detector distance produces low speckle noise levels. A sampling rate of 10 kSamples/s was also adopted, with a total observation period of 10 s. A multi-sine signal excitation was produced in order to tune the vibration response with the first four bending modes of the beam, as reported in Table 1.

Two sinusoidal line scan along the beam height were performed. These two scans differ only in terms of scanning frequency, i.e. 1 Hz and 10 Hz. These two scanning frequencies, a slower one and a faster one,

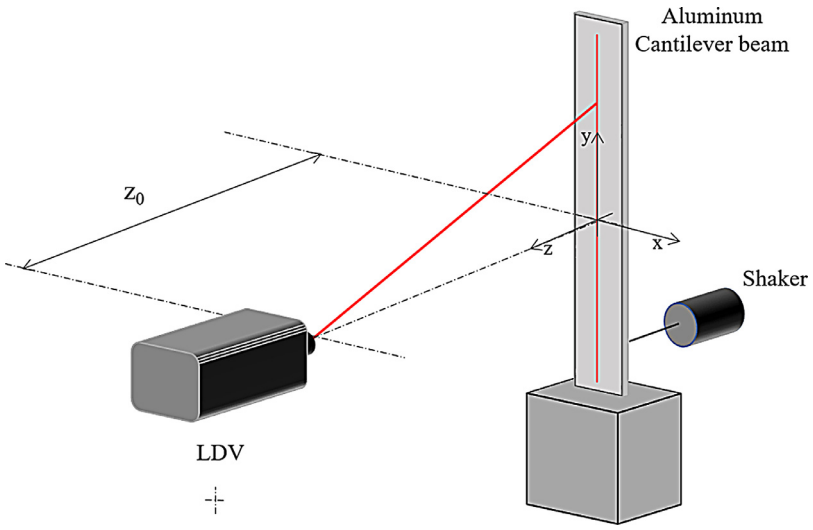

Fig. 6. Measurement setup for the clamped-free cantilever beam test.

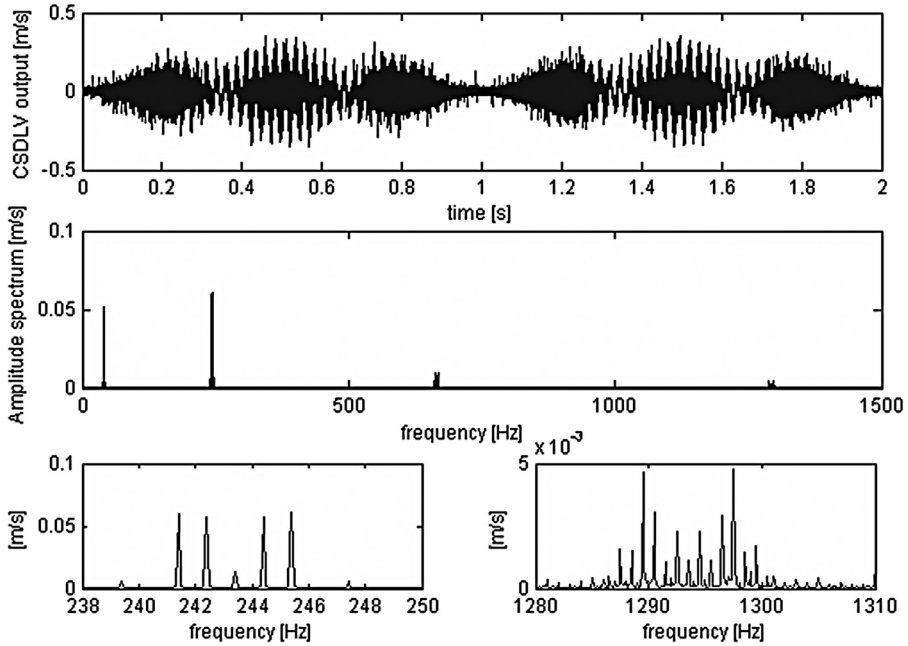

Fig. 7. CSLDV test on real data (Multi-sine Excitation): Acquired signal in the experimental test at 1 Hz of scanning frequency. Close-up on a time chunk of 2 s (top plot); vibration amplitude spectrum [0–1500 Hz] (central plot); vibration spectrum close-up around resonance frequency of mode II (bottom-left plot) and mode IV (bottom-right plot).

were tested in order to test the sensitivity of the algorithm to speckle noise increasing with the scan frequency.

Figs. 7 and 8 report the time histories, in a close up on a chunk of 2 s to better highlight amplitude modulation phenomena due to the ODSs excited, and the relative spectra of the signals acquired for the two scanning frequencies (1 Hz and 10 Hz, respectively). The signal acquired using a scanning frequency of 10 Hz shows a significant increase in the noise level. This is evident when observing the CSLDV spectral data, where speckle noise periodic nature clearly shows up. The sideband patterns of the four mode shapes are well separated for both the scan frequencies. They are visibly recognizable when the scan frequency is 1 Hz, see bottom plots of Fig. 7, where the sideband patterns of mode shapes II and IV are represented in the left and right plot, respectively. When the scan frequency is 10 Hz, the sideband pattern of mode shape II is still emerging from the noise pedestal while the sideband pattern of mode shape IV is buried into noise and it is not visibly recognizable any more. However, since noise is mainly periodic and the scan frequency and its harmonics do not coincide with the spectrum sidebands of mode shape IV, the algorithm is still able to correctly identify mode shape IV, as it will be shown below. The shape database is constituted by the first four clamped-free bending modes of the beam and the first 3 pinned-free bending modes of a beam of the same geometry. The insertion of these latter three modes ('fake' modes) is to test the approach in recognizing the right modes from those which cannot be associated to the target structure.

Fig. 9 reports the Euclidean distance of the set of candidate shapes for the two scan frequencies (1 Hz and 10 Hz). The lower distance associated to the 1 Hz scan frequency test is mainly due to a better SNR characterizing the signal. However, the difference between the Euclidean distance of the two tests is generally very small. Another trend is clearly evident:

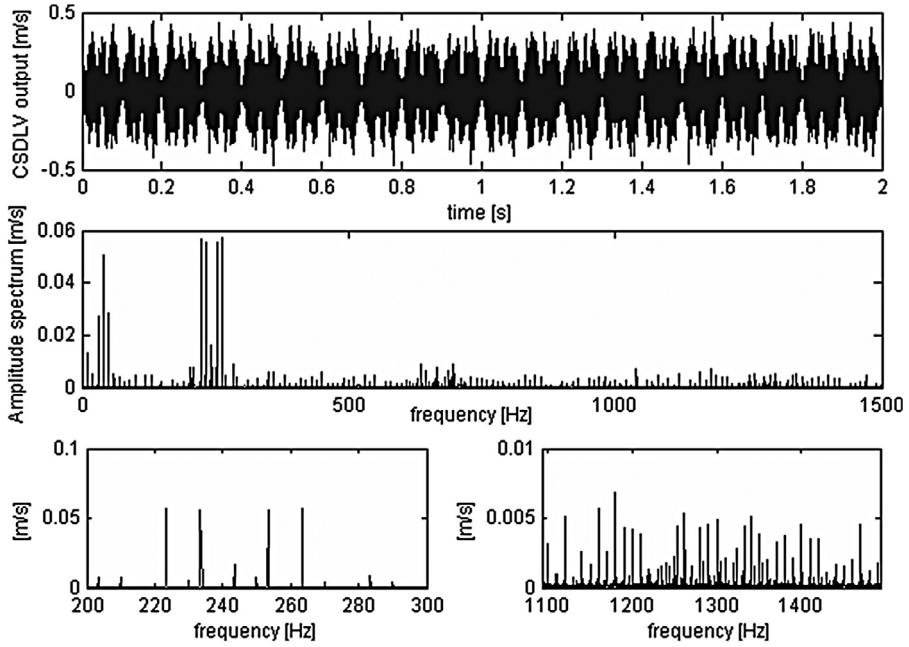

Fig. 8. CSLDV test on real data (Multi-sine Excitation): Acquired signal in the experimental test at 10 Hz of scanning frequency. Close-up on a time chunk of 2 s (top plot); vibration amplitude spectrum [0–1500 Hz] (central plot); vibration spectrum close-up around resonance frequency of mode II (bottom-left plot) and mode IV (bottom-right plot).

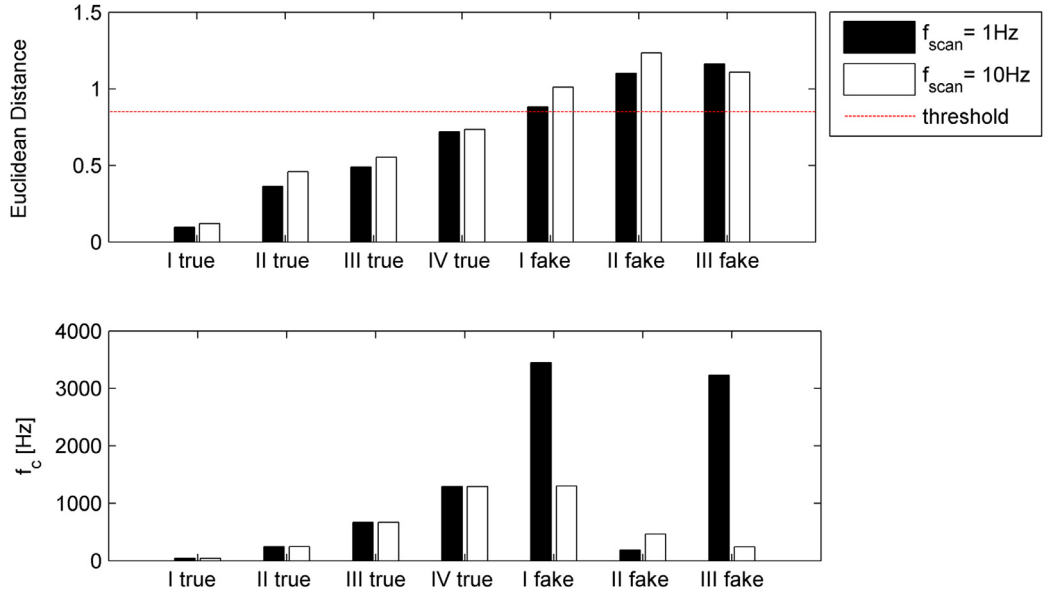

Fig. 9. CSLDV test on measured data: Euclidean distance and obtained mode frequencies for scanning frequencies of 1 Hz and 10 Hz.

the increase of the Euclidean Distance with the increase of mode shapes order. This is explainable considering that mode shapes of higher order generate as well sideband patterns of higher order. If the high order sidebands are buried into the noise, the algorithm suffers in classifying the correct shapes. However, all the four mode shapes effectively excited and generating the ODSs of the structure are correctly recognized by the algorithm. It is interesting to notice that the three mode shapes related to the pinned-free cantilever beam generate a quite large Euclidean distance. The Euclidean distance of the three fake mode shapes exceeds the threshold of 0.85, which has been considered as the minimum value to define the identification of a certain shape as an ODS present in the CSLDV spectrum. This is also in agreement with the recognizability limit distance discussed in Section 3.

Looking again at Fig. 9 it is also evident that fake mode shapes can be rejected by observing the central frequencies associated to the different shapes. As example, it is physically inconsistent that a first bending mode (see the 1st fake mode shape) takes place, in the structure tested, at a frequency of 1303 Hz. In addition, Fig. 9 compares results obtained using the two different scanning frequencies of 1 Hz and 10 Hz: if the behavior of the Euclidean distance is quite similar for the two cases, the same does not happen in terms of central frequencies. The frequencies obtained are not only not physically consistent, but also very different depending on the scanning frequency used. This happens because the kernel of a generic fake mode can find a quite good matching with the noise pattern, generally at higher frequencies.

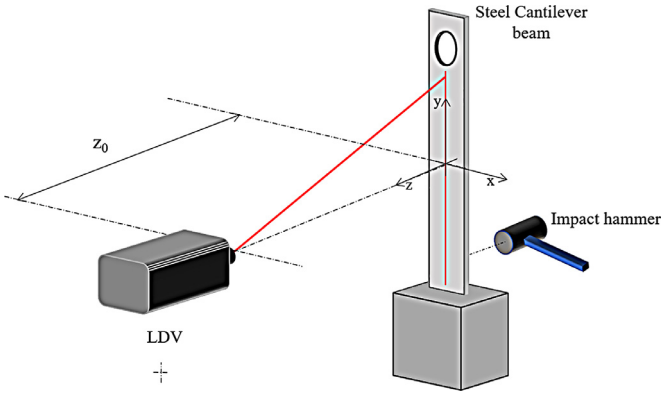

Fig. 10. Measurement setup for the clamped-free cantilever beam test.

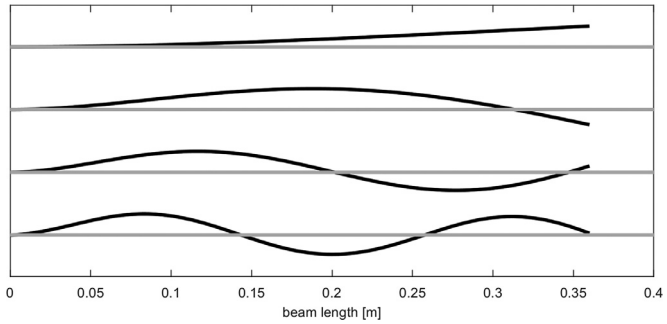

Fig. 12. Shape database for the Impact test analysis: beam shapes (black) and beam reference lengths (gray).

4.2. Transient excitation test

To show the potentials of the approach for general excitation sources, an experimental impact test has been performed on an steel clamped-free cantilever beam (height=0.4 m; width=0.04 m; depth=0.002 m). The beam is characterized by a hole (diameter=0.01 m) close to its free edge (hole center at 0.035 m from the free edge). The laser was placed (z_0) 2 m apart from the beam. A sinusoidal line scan along the beam height at half-width symmetry axis of the beam was performed. This choice was adopted to avoid torsional modes on the recorded vibration signal. The scan ranged from the clamped edge of the beam to the bottom part of the hole (Fig. 10). To challenge the approach also in case of strong speckle noise, a scan frequency of 15 Hz was adopted. This choice can be also necessary if the transient event has a short duration. The transient vibration response was sampled at a sampling rate of 8192 Samples/s, with a total observation period of 4 s. A Discrete Scanning (DSLDV) impact test was also performed to identify the reference resonance frequencies of the beam as well as its mode shapes progression. The measurement grid (12 points equally spaced) was set on the same line of the beam on which the CSLDV test was performed. Only the first four bending modes of the beam could be properly excited, they ranging in the frequency range 0–2 kHz. Measurement noise was too strong at higher frequency to extract valid mode shapes at higher frequency. For this reason, the analysis with the mode matching algorithm was also concentrated in this frequency range.

Fig. 11 shows the time history and the spectrum of the transient signal acquired. Speckle noise is well evident in the spectrum of the vibration signal.

The shape database was built using analytical formulation for a clamped-free beam considering the effective length of the scan and not the whole length of the beam. This results in the shapes reported in Fig. 12.

Table 2 reports the first four bending modes of the beam extracted from the analysis of the DSLDV impact test data and exploiting the mode matching approach. It can be seen that the algorithm well identifies both the mode shape order and their associated resonance frequencies. Two aspects come to sight when looking at the Euclidean distance values:

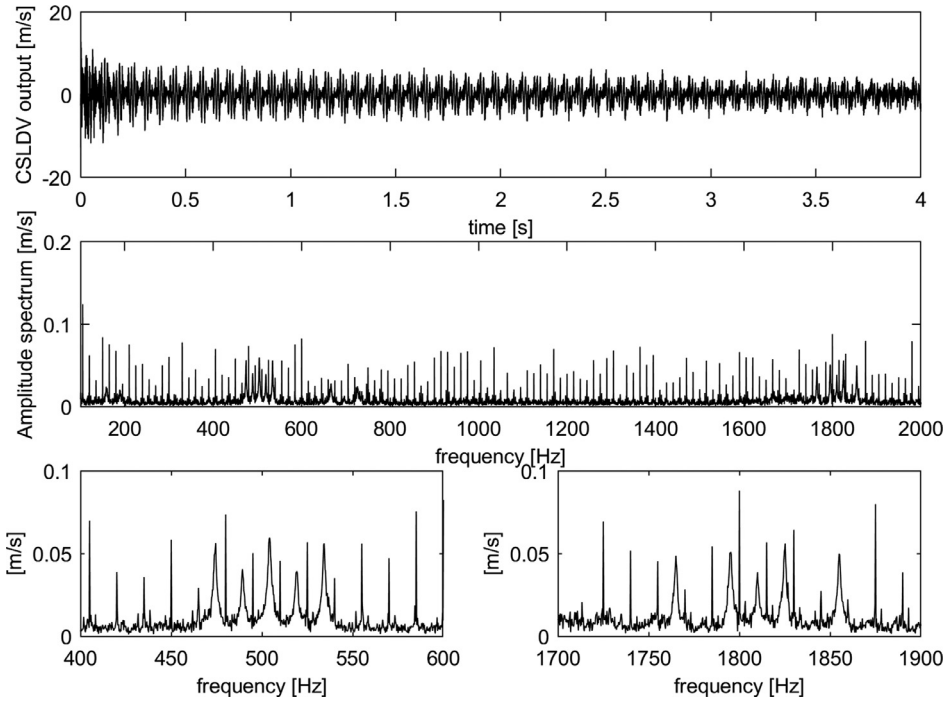

Fig. 11. CSLDV test on real data (Impact Excitation): Acquired signal in the experimental test at 15 Hz of scanning frequency. Time data (top plot); vibration amplitude spectrum [100–2000 Hz] (central plot); vibration spectrum close-up around resonance frequency of mode II (bottom-left plot) and mode IV (bottom-right plot).

Table 2
Resonance Frequencies and Euclidean Distance of the tested clamped-free cantilever beam: Impact excitation.

Mode shape	Resonance Frequency [Hz]		Euclidean Distance
	DSLDV Test	CSLDV test	
I	173.5	173.5	0.12
II	503	503	0.54
III	696	696	0.75
IV	1810	1810	0.65

- they are globally higher than those estimated in the multi-sine excitation test; this can be due to the higher speckle noise level;
- they increase as the shape index increases apart from mode III. This might be due to difficulty in properly exciting mode III which causes mode III high order sidebands to be buried in noise.This latter aspect could be tackled either decreasing the scan frequency or changing the excitation point.

It is well evident, however, that the approach performs well also on this challenging dataset.

5. Conclusions

CSLDV has represented an attractive alternative to the common Discrete Scan approach in vibration testing. Indeed, the possibility of extracting the ODSs of a structure reducing the measurement time and with a spatial resolution typically much higher than the one that can be adopted in Discrete SLDV mode with the same testing time, represents an undisputed appeal for a vibration testing measurement technique. The standard approach proposed by Ewins et al., however, grounds on the experience and the knowledge of the experimenter, who, starting from the visual inspection of the CSLDV spectrum, becomes able to extract the ODSs of the structure. The technique proposed in this paper reverses, in a certain way, the point of view of the experimenter who deals with CSLDV. The main assumption is based on the awareness that a mode shape produces a sideband pattern that is unique in nature. Therefore, it is not illogical to create a shapes database, with associated sideband patterns, and look for those patterns in the CSDLV spectrum exploiting a pattern matching approach. Those patterns that are found inside the spectrum represent the mode shapes/ODSs that best match with the ODSs which are effectively excited during the vibration test.

The sensitivity of the method to various parameters that can affect its performance has been discussed. Moreover, its effectiveness was proved on real vibration data measured on a clamped-free aluminum cantilever beam. With respect to its sensitivity to random and periodic noise, it has been shown that the presented approach is more sensitive to periodic noise (SNR limit 0 dB in case of periodic noise with respect to −17 dB shown in case of random noise) when the central frequency of a certain ODS coincides with an integer multiple of the scanning frequency used to perform the test. The sensitivity to close resonance frequencies (uncoupled-close mode shapes) has been tested. It has been demonstrated that the method accurately distinguishes and separates uncoupled-close mode shapes unless the sideband patterns of the two mode shapes are modified by the superimposition of certain sidebands. The same holds for the case of coupled-close mode shapes.

The method has been applied on two different experimental datasets. The first dataset refers to experimental CSLDV vibration data collected on an aluminum clamped-free cantilever beam. It has been proved that the proposed approach can easily identify the ODSs that were excited during the vibration tests and that it is also able to separate those ODSs from a set of “fake” mode shapes that were added on purpose to make things harder for the pattern recognition algorithm. Extremely good results have been obtained at both low (1 Hz) and high (10 Hz) scanning frequencies, showing the applicability of the technique also on data characterized by a poor SNR. The second dataset refers to an impact test performed on a clamped-free steel beam. This second dataset was chosen to prove the applicability of the method on a more general excitation condition (e.g.transient excitation) requiring high scan rate (15 Hz in the test discussed in the paper) because of the duration of the phenomenon. The approach resulted to be robust enough to properly identify the shapes and their associated resonance frequencies even in such challenging conditions.

More work is required to carry the technique to a processing method exploitable in daily testing, such as testing on complex modes, database filled with numerical models from Finite Element analyses etc. However, the premises are good enough to state that the method represents a first step towards an automation of CSLDV processing.

References

[1] Sriram P, Craig JI, Hanagud S. Scanning laser doppler vibrometer for modal testing. Int J Anal Exp Modal Anal 1990;5:155–67.
[2] Stanbridge AB, Martarelli M, Ewins DJ. Measuring area mode shapes with a scanning laser Doppler vibrometer. In: Proceedings of the international modal analysis conference - IMAC XVII; 1999. p. 980–5.
[3] Stanbridge AB, Martarelli M, Ewins DJ. Measuring area vibration mode shapes with a continuous-scan LDV. Meas J Int Meas Confederation 2004;35(2):181–9.
[4] Stanbridge AB, Martarelli M, Ewins DJ. The scanning laser Doppler vibrometer applied to impact modal testing. In: Proceedings of 17th international modal analysis conference (IMAC XVII), Orlando; 1999.
[5] Vanlanduit S, Guillaume P, Schoukens J. Broadband vibration measurements using a continuously scanning laser vibrometer. Meas Sci Technol 2002;13(10):1574–82.
[6] Martarelli M, Castellini P, Santolini C, Tomasini EP. Laser Doppler vibrometry on rotating structures in coast-down: resonance frequencies and operational deflection shape characterization. Meas Sci Technol 2011;22:115106.
[7] Martarelli M, Castellini P. Performance analysis of continuous tracking laser Doppler vibrometry applied to rotating structures in coast-down. Meas Sci Technol 2012;23:065202.
[8] Allen MS, Sracic MW. Mass normalized mode shapes using impact excitation and continuous-scan laser Doppler Vibrometry. Italian association of laser velocimetry and non-invasive diagnostics (AIVELA), Ancona, Italy; 2008.
[9] Allen MS, Sracic MW. A method for generating pseudo single-Point FRFs from continuous scan laser vibrometer measurements. 26th international modal analysis conference (IMAC XXVI), Orlando, Florida; 2008.
[10] Allen MS. Continuous-scan vibrometry technique for broadband vibration measurements with high spatial detail. J Acoust Soc Am 2009;126(4):2255.
[11] Chiariotti P, Martarelli M, Revel GM. Exploiting continuous scanning laser Doppler vibrometry (CSLDV) in time domain correlation methods for noise source identification. Meas Sci Technol 2014;25.
[12] Chiariotti P, Revel GM, Martarelli M. Delamination detection by multi-Level wavelet processing of continuous scanning laser doppler vibrometry data. Opt Lasers Eng 2017. ISSN 0143–8166. doi: 10.1016/j.optlaseng.2017.01.002.
[13] Chiariotti P, Martarelli M, Castellini P. Exploiting continuous scanning laser doppler vibrometry in timing belt dynamic characterisation. Mech Syst Signal Process 2017;86:66–81. doi:10.1016/j.ymssp.2016.01.001.
[14] Salman M, Sabra KG. Synchronized vibrations measurements at multiple locations using a single continuously scanning laser Doppler vibrometer. applications to non–contact sensing of human body vibrations. J Acoust Soc Am 2011;130(4):2394.
[15] Aranchuk V, Lal AK, Zhang H, Hess CF, Sabatier JM. Acoustic sensor for landmine detection using a continuously scanning multi-beam LDV. In: Proceedings of the SPIE, Orlando, vol. 5415; 2004. p. 61.
[16] Chiariotti P, Castellini P, Martarelli M. Recovery of mode shapes from continuous scanning laser doppler vibration data: a mode matching frequency domain approach. Topics in modal analysis I, Volume 7 Conference proceedings of the society for experimental mechanics series. De Clerck J, editor. Cham: Springer; 2014.
[17] Vlachos M, Gunopoulos D, Kollios G. Discovering similar multidimensional trajectories. In: Proceedings of the 18th international conference on data engineering, ICDE ’02. Washington, DC, USA: IEEE Computer Society; 2002.
[18] Goldin DQ, Millstein TD, Kutlu A. Bounded similarity querying for time-series data. Inf Comput 2004;194(2):203–41.
[19] Blevins RD. Formulas for natural frequencies and mode shape. Robert E. Krieger Publishing Co. Inc.; 1984.
[20] Martarelli M, Ewins DJ. Continuous scanning laser Doppler vibrometry and speckle noise occurrence. Mech Syst Signal Process 2006;20(8):2277–89.
[21] Sracic MW, Allen MS. Experimental investigation of the effect of speckle noise on Continuous Scan Laser Doppler Vibrometer measurements. Proceeding of the 27th international modal analysis conference, Orlando; 2009.